Am J Transl Res 2016;8(12):5271-5285
www.ajtr.org /ISSN:1943-8141/AJTR0038289

Original Article

Endogenous nitric oxide regulates blood vessel growth factors, capillaries in the cortex, and memory retention in Sprague-Dawley rats

Sanrong Wang[1], Yingqiang Qi[2,3], Lehua Yu[1], Lei Zhang[2,3], Fenglei Chao[2,3], Wei Huang[2,3], Rongzhong Huang[1], Hongxu Li[1], Yanming Luo[2,3], Yun Xiu[2,3], Yong Tang[2,3]

[1]Department of Rehabilitation Medicine and Physical Therapy, Second Affiliated Hospital, Chongqing Medical University, Chongqing, P. R. China; [2]Department of Histology and Embryology, Chongqing Medical University, Chongqing, P. R. China; [3]Laboratory of Stem Cell and Tissue Engineering, Chongqing Medical University, Chongqing, P. R. China

Received May 9, 2016; Accepted November 27, 2016; Epub December 15, 2016; Published December 30, 2016

Abstract: The effects of nitric oxide (NO) on cerebral capillary angiogenesis and the regulation of pro- and anti-angiogenic factors that affect cerebral capillary angiogenesis, spatial learning, and memory ability are unclear. We assessed the effects of the NO precursor L-arginine (L-ARG) and the NO synthesis inhibitor Nω-nitro-L-arginine methylester (L-NAME) on cortical capillaries and spatial learning and memory abilities. We administered intracerebroventricular injections of L-ARG or L-NAME to rats before they were evaluated in the Morris water maze. We measured the levels of NO synthase activity, pro-angiogenic factors, vascular endothelial growth factor (VEGF), basic fibroblast growth factor (FGF-2), and the expression of the anti-angiogenic factors angiostatin and endostatin. We also quantitatively investigated parameters of the cortical capillaries using immunohistochemistry and stereological methods. The L-ARG treatment significantly improved rats' spatial learning abilities and increased NOS activity in the cortex. L-NAME disrupted spatial learning. Following the L-ARG treatment, the expression of the pro-angiogenic factors (VEGF and FGF-2) was higher and the expression of anti-angiogenic factors (endostatin) was lower than the vehicle-treated animals. In contrast, the L-NAME treatment reduced the expression of VEGF and increased the expression of endostatin. Based on these results, modulation of the NO content in the brain regulates VEGF, FGF-2, and endostatin expression, as well as capillary parameters in the cortex, which in turn influence spatial learning and memory performance.

Keywords: Nitric oxide, spatial learning and memory, angiogenesis, pro- and anti-angiogenic factors, stereology

Introduction

Angiogenesis is defined as the formation of new blood vessels that grow from endothelial cell aggregates in mammalian embryos. During this process, the formation of the vascular plexus by endothelial progenitor cells is called vasculogenesis [1-3]. According to the vascular niche hypothesis, an angiogenic environment is also required for the generation, regeneration and repair of neurons during adult neurogenesis [4, 5]; therefore, angiogenesis is particularly important in brain function research. Both genetic mechanisms and blood vessel growth factors in the local micro-environment regulate angiogenesis [1-3]. Blood vessel growth factors are divided into pro- and anti-angiogenic factors, and the balance between these two factors determines the extent of blood vessel growth [6].

Pro-angiogenic factors promote the proliferation and migration of vascular endothelial cells, matrix protein lysis, and the formation of new capillary structures. These factors also exert a catalytic role in the proliferation and secretion of vascular smooth muscle cells and perivascular stromal cells. Previous studies have identified ten species of pro-angiogenic factors, which include strong effectors such as VEGF and FGF-2. VEGF was initially identified as a tumor secretion-promoting factor when it was

applied to endothelial cells [7], neuronal cells [8], and tumor cells [9]. FGF-2 modulates the pleiotropic effects of different cell and tissue systems. Both low and high molecular weight variants of FGF-2 promote vascular growth [10]. In addition, the FGF-2 and VEGF signaling pathways may coordinate to promote angiogenesis [11-17].

Anti-angiogenic factors, such as endostatin and angiostatin, negatively regulate the proliferation and migration of vascular endothelial cells during angiogenesis either directly or by opposing the action of pro-angiogenic factors. Endostatin inhibits the expression of genes that are normally stimulated by VEGF and FGF-2, including hypoxia-inducible factor subunit 1α (HIF-1α) [18]. Endostatin also effectively inhibits the formation of microvessels and mainly acts at the level of neovascularization; however, it also has a weaker effect on existing vessels [19, 20]. Angiostatin utilizes a mechanism that is similar to endostatin; it blocks the phosphorylation of focal adhesion kinase by binding to integrin α5β1 to effectively block the VEGF pathway. This blockade inhibits the Wnt signaling pathway and deactivates matrix metalloproteinases. When angiostatin binds to the cell membrane, annexin, angiomotin, integrin αvβ3, and other proteins affect the cell's ability to inhibit angiogenesis [21]. Angiostatin regulates the expression of anti-angiogenic factors and proapoptotic pathways and targets the mitochondrial Kringle active region. In addition, angiostatin can selectively bind to ATP synthase, which inhibits the proliferation and migration of endothelial cells [22].

Nitric oxide (NO), a free radical gas produced by the NO synthase (NOS) protein family, plays an important role in several brain functions and related clinical conditions, including the regulation of neuronal excitability, synaptic plasticity, long-term potentiation, long-term depression, neurotoxicity, and neuroprotection [23, 24]. NO is also a ubiquitous second messenger in various physiological responses in the vascular system, including the processes of vasodilation, anti-coagulation, vascular remodeling and angiogenesis. NOS inhibitors were used to show that endothelial NOS, cytokine-inducible NOS, and neuronal NOS play roles in the formation of the vascular system. As shown in previous studies, NO acts as a master regulator of other pro-angiogenic factors such as VEGF and FGF-2, as well as anti-angiogenic factors such as endostatin and angiostatin [25-27]. However, NO is a compound with a narrow therapeutic window; specifically, the effects of NO-related compounds depend on the concentration, time, and treatment conditions. Excessive NO production may induce neurotoxicity, particularly in the presence of oxidative stress, since NO may react with superoxide to form peroxynitrite [28]. Therefore, the manipulation of the NO signaling pathway using low levels of these compounds may affect downstream angiogenesis regulators in the cortex.

The cortex is one of the most important structures in the brain and plays a role in spatial learning and memory. However, researchers have not yet examined the effects of NO on cognitive ability and cortical capillaries. Additionally, researchers do not yet know whether NO regulates angiogenesis in the cortex and if this process occurs through an interaction with other pro- and anti-angiogenic factors. In this study, we investigated the effects of intracerebroventricular (i.c.v.) administration of the NO precursor L-ARG or the NOS inhibitor L-NAME on NOS activity and angiogenesis in the cortex. We used the Morris water maze to test spatial learning and memory ability and immunohistochemistry and stereological methods to assess the effects of NO on the total length, total volume and total surface area of capillaries in the cortex. Finally, we employed real time-PCR and western blots to investigate the effects of NO on the expression of the pro-angiogenic factors VEGF and FGF-2 and the anti-angiogenic factors angiostatin and endostatin in the cortex.

Materials and methods

Animals

Eight-week old male Sprague-Dawley rats that weighed 280-320 g were obtained from the laboratory animal center of Chongqing Medical University, P. R. China (75 rats). The animals were housed at the laboratory animal center of Chongqing Medical University and maintained at a controlled temperature (22 ± 2°C) on a 12-h light/dark cycle. Three or 4 rats were housed in one standard plastic cage with free access to food and water. The Sprague-Dawley rats were randomly divided and assigned to the

L-ARG (n = 25), L-NAME (n = 25), or the normal saline (NS) (n = 25) groups. The number of rats that were excluded from each group due to an anesthetic accident, infection, or other causes included 3 (12%) in the NS group, 6 (24%) in the L-ARG group, and 5 (20%) in the L-NAME group. All procedures were conducted in accordance with the Guide for the Care and Use of Laboratory Animals from the National Institutes of Health (NIH).

Surgery and model construction

One week before the commencement of the experiments, animals were intraperitoneally injected with 1% pentobarbital sodium (Sigma, Germany), 0.4 ml/100 g, to induce anesthesia. Polyethylene cannulae (PE-10, OD 0.6 mm, ID 0.3 mm; Rivard Technology Co, China.) were implanted according to the coordinates in the Paxinos rat brain stereotaxic atlas [29]. The cranium was exposed, and a cannula was implanted into the right lateral ventricle 3.8 mm below the surface, 1.3 mm to the right of the sagittal suture, and 0.8 mm behind the coronal suture. The cannula was attached to the skull with dental cement. The rats were allowed to recover and received food and water ad libitum for 1 week; buprenorphine was provided prophylactically for pain relief for a minimum of 2 days post surgery. Only animals that exhibited normal motor functions were used in the subsequent experiments after the recovery period. These rats were randomly divided into three groups (25/group). Animals in two groups received i.c.v. injections of 5 μl of L-ARG (0.5 μmol/day; L-ARG group) [30] or L-NAME (5 μmol/day; L-NAME group) [31] for 28 days, followed by 5 μl of saline to flush the catheter. The same amount of normal saline was administered to the controls (NS group). The drugs were diluted in physiological saline (0.9% w/v). L-ARG (A5006) and L-NAME (N5751) were purchased from Sigma (USA).

Morris water maze test

A circular pool (1.5 m in diameter) connected to an automatic track and analysis system (SLY-R01& WMS, Beijing Sunny Instruments Co. Ltd., Beijing, China) was used for the experiment. The water was blackened with ink, and a controlled temperature (22 ± 2°C) was maintained during the test. Each rat was tested in four different quadrants labeled A, B, C and D. The start position of the four experiments was the same each day, and the order of the starting position was the same in the four experiments for all animals on the same day. However, the order of the start position was randomly determined each day. The rats were slowly placed in the water facing the wall of the pool. A visible platform was used on the first day, and a hidden platform was used on the next five days. The platform remained in the same quadrant for six days. In each experiment, the animals were allowed to swim for 120 s until it located the platform and were allowed to remain on the platform for 15 s. If the rat did not locate the platform within 120 s, it was guided to the platform and allowed to remain on the platform for 15 s. The interval time between subsequent experiments was more than 15 min for each animal. Twenty-four hours after the last training session on the seventh day, the platform was removed. The two farthest points from the platform were selected as the two entry points. Rats were allowed to perform two probe trials, and performed a free swim for 120 s per trial. The time and the distance required to reach the platform (escape latency) and the target zone frequency were automatically recorded by a video tracking system [32, 33].

NOS activity

The cortex was homogenized on ice in 10 volumes of 0.9% saline. The homogenate was then centrifuged at 2,000 rpm for 10 min at 4°C, and NOS activity in the supernatant was determined according to the instructions included in the total Nitric Oxide Synthase assay kit (A014-2; Nanjing Jiancheng Bioengineering Institute, China). We tested the NOS activity by measuring the optical density (OD) at a wavelength of 530 nm using a 752-UV grating spectrophotometer (Amersham Biosciences, USA). The OD value of ddH_2O, a blank, was determined. The protein concentration in the sample was determined using Coomassie brilliant blue G-250, with bovine serum albumin as the standard. The total NOS activity in the cortical homogenates was calculated using the following equation: $Total_{\text{-}NOS}(U/ml) = ({}^{OD}_{tNOS} - {}^{OD}_{tNOS\ Blank})/1000$ (nanomolar extinction coefficient of chromophore at 530 nm) (light path(1) × reaction time(15)) × *total* volume of the reaction solution (ml)*/volume* of the sample used (ml).

Perfusion and estimation of cortical volume

After the spatial learning and memory tests, five male and five female rats were randomly selected from each of the three groups. The rats were deeply anesthetized via an intraperitoneal injection of 1% pentobarbital sodium (0.4 ml/100 g) (Sigma, Germany). The tissues from the rats were subsequently perfused with 100 ml of 4% paraformaldehyde in 0.6 M phosphate-buffered saline (pH 7.4). The cerebellum, brain stem, cranial nerves, which are located under the pavimentum cerebri, and cerebral hemispheres were removed after the perfusion. The hemispheres were embedded in 6% agar and cut into 1-mm-thick coronal slices beginning at the rostral pole.

The slices were photographed under an anatomical microscope at 10 × magnification. A transparent plastic sheet marked with equidistant points was randomly placed on the caudal surface of each photographed slab, and the points that appeared within the cortex were then counted. The cortical volume was calculated using the following previously described equation [34, 35]:

$$Vcortex = t \times a(p) \times \sum Pcortex$$

where Vcortex indicates the total volume of the cortex, t indicates the slab thickness (1 mm), (p) indicates the area associated with each grid point (0.06 mm^2), and ∑Pcortex indicates the total number of grid points that appeared within the cerebral cortex in each rat.

Cortical sampling

After the total volume of the cortex was measured, every three slices were randomly sampled, and the first slice was selected from the first three slabs. Equidistant light points were randomly projected onto the occipital surface of the sampled slices. Tissue blocks of approximately 1 mm^3 were cut from the cortex in the region where the points on the plastic sheet appeared within the cortex. Five to 6 blocks were sampled per rat.

Randomly selected slices of the hemisphere were postfixed in 4% paraformaldehyde for more than two hours. The samples were subsequently embedded in agar with the caudal surface facing down. The embedded samples were treated with the isector technique to obtain isotropic, uniform random (IUR) sections [35, 36]. After the IUR surface was obtained, one section with a thickness of 5 μm was cut from each block along the direction parallel to the IUR surface. The 5-μm sections were referred to as the IUR sections. The isector technique ensures that the capillaries have the same probability of being sampled in each direction of the three-dimensional space.

Immunohistochemistry procedure

The sections were immersed in citrate buffer (0.01 M, pH 6.0) and then microwaved for 15 min for antigen retrieval. After cooling, the sections were washed twice in PBS (0.01 M, pH 7.4) and then soaked in 3% hydrogen peroxide for 10 min at room temperature to inactivate endogenous peroxidases. Next, the sections were washed three times in PBS for 5 min prior to incubation with 5% goat serum for 20 min at room temperature to prevent nonspecific staining. Then, the sections were incubated with a 1:200 dilution of the rabbit polyclonal anti-collagen IV primary antibody (ab6586; Abcam, Cambridge, UK) in PBS overnight at 4°C, followed by a 1-h incubation at 37°C. Afterwards, the sections were washed three times in PBS for 5 min. The sections were transferred to a secondary antibody solution (biotinylated goat-anti-rabbit immunoglobulin G) and incubated for 20 min at 37°C. The specimens were incubated with horseradish peroxidase-conjugated streptavidin (S-A/HRP) for 20 min at 37°C, followed by three washes in PBS for 5 min. The sections were then transferred to a diaminobenzidine (DAB) solution (ZLL-9032, Beijing, China), which was used as the chromogen, and were incubated for approximately 10 min. The sections were dehydrated in a graded ethanol series and xylene by sequential immersion, covered with a cover slip, and viewed under a light microscope (Olympus, Tokyo, Japan). Four to six fields of view of the cortex were randomly captured in each section under a 100 × oil objective lens (Olympus, Tokyo, Japan). The vessels with a luminal diameter less than 10 μm were defined as capillary net components [32, 37].

Analysis of the images of cortical capillaries

An unbiased counting frame was randomly superimposed on each captured photograph

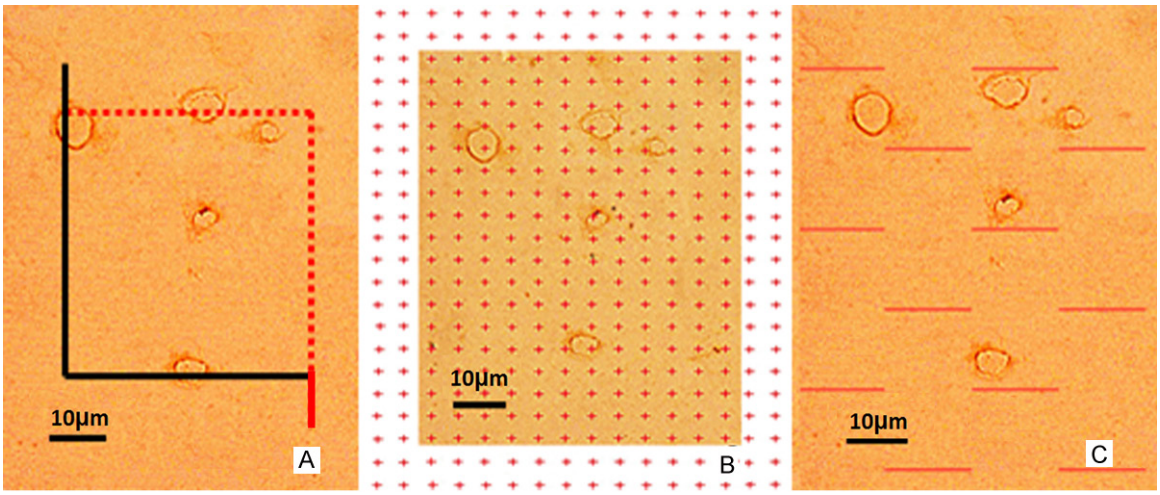

Figure 1. A. Unbiased counting frame placed on a randomly captured image. Capillary profiles were counted if they were located completely inside the counting frame or were located partially inside it and were still touching the counting lines (dotted lines). Capillary profiles were excluded if they touched the exclusion lines (solid lines). B. Points that were located in the cortex and capillary profiles were counted. C. Intersection points between the test lines and the capillary luminal surface were counted. Scale bar = 10 μm.

Table 1. Primer sequences used for real-time quantitative PCR

Primer name	Sequence 5' to 3'	Primer type
VEGF	5' ACGTCTACCAGCGCAGCTATTG 3'	Forward
	5' ACGCACTCCAGGGCTTCATC 3'	Reverse
FGF-2	5' GGACGGCTGCTGGCTTCTAA 3'	Forward
	5' GCCCAGTTCGTTTCAGTGCC 3'	Reverse
Angiostatin	5' AGGTGGAGCCGAAGAAATGC 3'	Forward
	5' CTGGGGATATTAAAGTACCGCC 3'	Reverse
Endostatin	5' TGTGCCCATCGTCAACCTG 3'	Forward
	5' GCCATGCCATACGCTCTTCT 3'	Reverse
β-Actin	5' CCGTAAAGACCTCTATGCCAAC 3'	Forward
	5' ACTCATCGTACTCCTGCTTGCT 3'	Reverse

(**Figure 1A**). The length density of the cerebral cortical capillaries was estimated with a stereological method previously described [32, 37]: *Lv(cap/cortex) = 2 × SQ(cap)/ΣA(frame).*

Where SQ(cap) denotes the total number of the capillary profiles counted per rat cortex, and ΣA(frame) is the total area of counting frames per rat. The total length of the cortical capillaries equaled the cortical volume, Vcortex, multiplied by the length density of the cortical capillaries, Lv(cap/cortex).

A transparent point grid was randomly placed on the photographs. The points that intersected with the capillaries, SP(cap), and the points that intersected with the cortex, SP(C), were counted (**Figure 1B**). The volume density of the cortical capillaries, Vv(cap/cortex), was calculated using the following equation [32, 37]: *Vv(cap/cortex) = SP(cap)/SP(C).*

The volume density of the cortical capillaries, Vv(cap/cortex), multiplied by the cortical volume (Vcortex) yielded the total volume of the cortical capillaries [32, 37].

Test lines were randomly placed on each photograph. The intersection points between the test lines and the capillary luminal surface, SPI (cap), and the total length of the lines that intersected with the cortex, ΣL(C), were recorded (**Figure 1C**). The surface area density of the cortical capillaries, Sv(cap/cortex), was estimated using the following equation [32, 37]: Sv(cap/cortex) = 2 × SPI(cap)/ΣL(C).

The surface area density of the capillaries, Sv(cap/cortex), multiplied by the cortical volume (Vcortex) represented the total surface area of the cortical capillaries [32, 37].

RNA preparation and real-time quantitative PCR analysis

Total RNA was isolated from the cortical tissues using Trizol reagent (Boxiang Biotechnology),

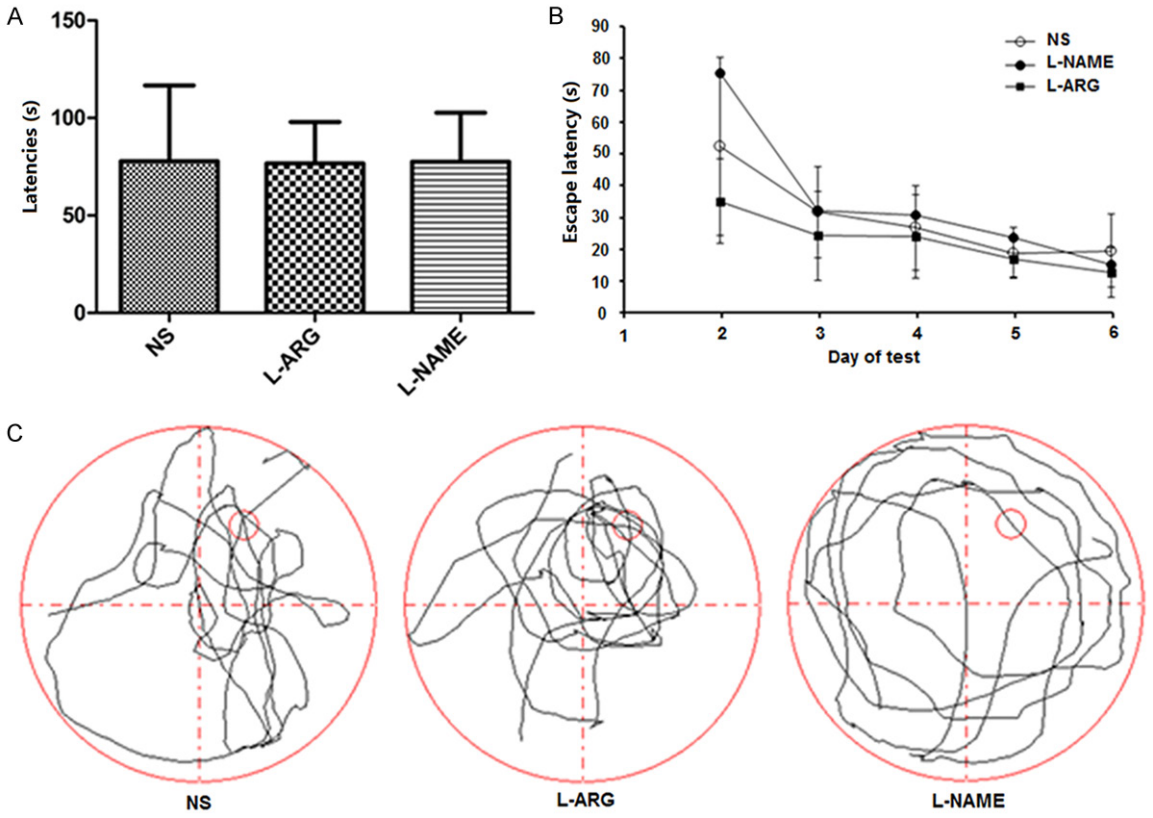

Figure 2. A. Mean escape latency of each group on the first day of the visible platform test (mean ± SD). B. Escape latencies among the groups on the second to the sixth days were measured using the Morris water maze test. C. Tracings of the typical swim patterns observed in the probe trials; the small circle indicates the position of the escape platform.

and cDNAs were synthesized from total RNA using Superscript II reverse transcriptase (RR820A, Takara Biotechnology). For each new RNA sample, two controls were established, a no template control and a no enzyme control, in which sterile water replaced the omitted enzyme or RNA. The cDNAs were amplified by qRT-PCR using primers (**Table 1**) specific for VEGF, FGF-2, endostatin and angiostatin (RNA polymerase II largest subunit). The reaction mixture consisted of 2 μl of cDNA product, 0.25 μl of the forward and reverse primers (2.5 M), 12.5 μl of iQ™SYBR® Green Supermix (Takara Biotechnology), and 10 μl of RNase/DNase-free dH_2O. The qRT-PCR conditions were set on the Quantitative Real-Time PCR thermocycler (Bio-Rad) as follows: 95°C for 10 min, followed by 45 cycles, each consisting of 95°C for 20 s, 60°C for 18 s, and 72°C for 30 s. Once the amplification cycles were completed, melting curves were generated by performing an additional cycle to verify the amplification of one gene per primer pair. Primers were designed to span exons to eliminate genomic DNA amplification. Gene expression was normalized to a control reference gene using the CT method [38].

Western blotting

Protein samples were generated from the cortex, separated on polyacrylamide gels, and transferred to nitrocellulose membranes as previously described [39, 40]. The nitrocellulose membranes were blocked for one hour in blocking buffer (5% milk, 5% BSA, and 0.1% Tween in PBS). The membranes were then incubated with 1:400 dilutions of the following primary antibodies overnight at 4°C: VEGF (ab-9570, Abcam Biotechnology), FGF-2 (ab-1062-45, Abcam Biotechnology), endostatin (sc-25720, Santa Cruz Biotechnology), and angiostatin (ab-2904, Abcam Biotechnology). The membranes were also incubated with an anti-β-actin antibody (1:500, D160117, Santa Cruz Biotechnology) to confirm equal protein load-

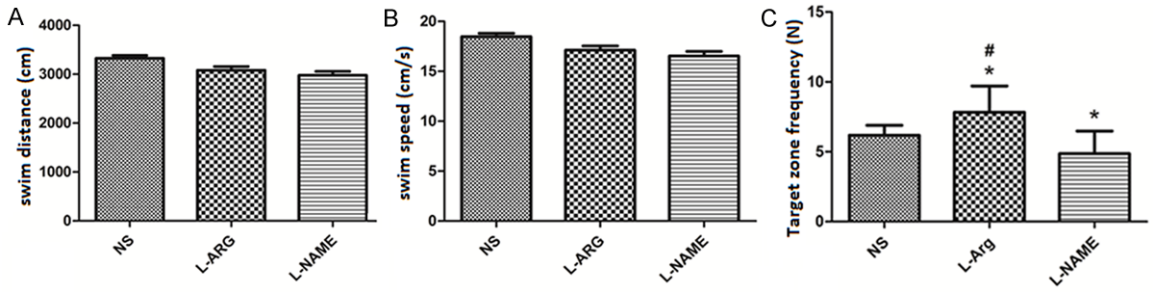

Figure 3. Swim distance, swim speed and target zone frequency of each group measured in the Morris water maze test (mean ± SD). *indicates $P < 0.05$ vs. NS. #indicates $P < 0.05$ vs. L-NAME.

ing. After incubation, the membranes were washed three times (10 min each wash) with wash buffer (0.1% Tween in PBS) and then incubated with 1:1,000 dilutions of horseradish peroxidase-conjugated anti-rabbit antibodies in blocking buffer for 1 h. The blots were washed three times in wash buffer, and ECL reagent (Millipore, Biosciences) was used to detect the peroxidase signals in the blot, according to the manufacturer's instructions. Densitometric quantification of the immunoreactivity was performed with a computerized image analysis system (Bio-Rad, USA). We treated all gels the same way and all western blot experiments were repeated at least three times. The integrated optical density of the bands was corrected by subtracting the background values. The ratios of the proteins of interest to β-actin were expressed as a percentage of the average of the control in each blot.

Statistical analysis

Quantitative data are expressed as the means ± standard deviations (SD); the statistical significance of the differences in spatial learning ability were analyzed using a repeated measures analysis of variance (ANOVA). One-way ANOVA followed by Tukey's test was used to determine the significance of the differences in all other parameters. Statistical analyses was performed with SPSS 17.0 software. A p value of < 0.05 was considered statistically significant.

Results

Effects of NO on spatial learning ability

We injected the rat cortices with the NO precursor L-ARG and the NOS inhibitor L-NAME to understand how NO influenced spatial learning. We did not observe a significant difference in the escape latency among the three groups ($P > 0.05$) (**Figure 2A** and **2B**). Rats in the L-ARG-treated group spent slightly more time in the correct quadrant than in the other three quadrants compared to the control group, whereas rats in the L-NAME group spent less time in the correct quadrant (**Figure 2C**). Although there was no significant difference in the swimming distance and swimming speed among the three groups ($P > 0.05$) (**Figure 3A**, **3B**), the target zone frequency of the L-ARG group was significantly increased when compared to the NS and L-NAME groups. The target zone frequency of the L-NAME group was significantly decreased compared to the NS group ($P < 0.05$) (**Figure 3C**).

NOS activity in the cerebral cortex

We monitored NOS activity in the treated animals to evaluate the effects of L-ARG and L-NAME on NO production. NOS activity was significantly increased in the cerebral cortex of animals the L-ARG group compared to the animals in the L-NAME and NS groups ($P < 0.05$). Conversely, the animals in the L-NAME group displayed significantly reduced NOS activity compared to the animals in the NS group ($P < 0.05$) (**Figure 4A**).

Cortical volume

We also measured the cortical volumes in the rats from the three groups. The mean volume of the cerebral cortex was 601.9116 ± 26.33 mm^3 in the NS group, 544.12 ± 59.91 mm^3 in the L-ARG group, and 549.47 ± 26.29 mm^3 in the L-NAME group, with no significant differences among the three groups ($P > 0.05$) (**Figure 4B**).

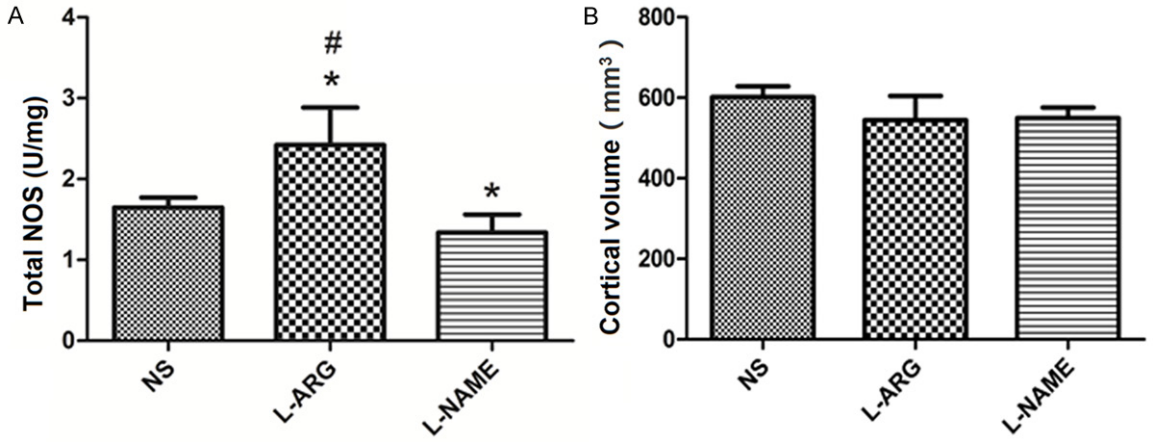

Figure 4. A. NOS activity in the cortex (mean ± SD). *indicates $P < 0.05$ vs. NS, #indicates $P < 0.05$ vs. L-NAME. B. Cortical volumes (mean ± SD).

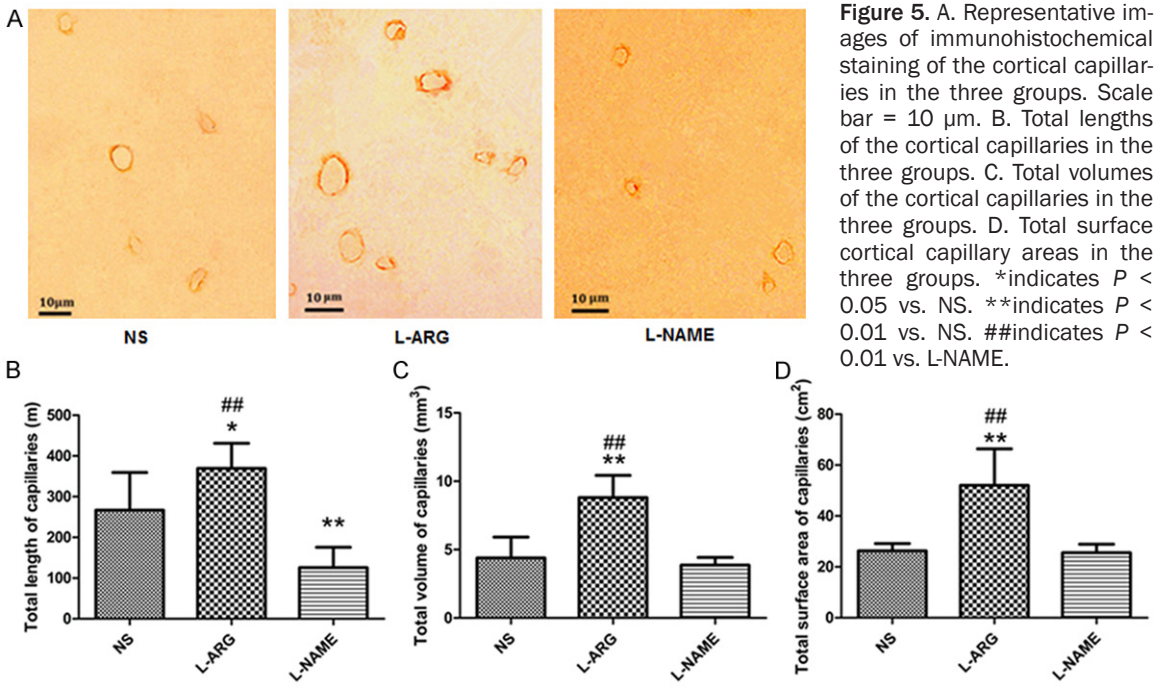

Figure 5. A. Representative images of immunohistochemical staining of the cortical capillaries in the three groups. Scale bar = 10 μm. B. Total lengths of the cortical capillaries in the three groups. C. Total volumes of the cortical capillaries in the three groups. D. Total surface cortical capillary areas in the three groups. *indicates $P < 0.05$ vs. NS. **indicates $P < 0.01$ vs. NS. ##indicates $P < 0.01$ vs. L-NAME.

Cortical capillaries

Immunohistochemistry of the cortex capillaries: We performed immunohistochemical staining with anti-collagen IV antibodies on the cortical capillaries and imaged them with a microscope to assess the effects of the treatments on the cortical capillary network (**Figure 5A**).

Stereological analysis of the cortical capillaries

Cortical capillary length: Using the images obtained from immunohistochemical staining, we calculated the average length of the cortical capillaries as 266.97 ± 92.51 m in the NS group, 369.25 ± 61.88 m in the L-ARG group, and 125.64 ± 50.06 m in the L-NAME group. The length of the cortical capillaries in the L-ARG group was significantly increased compared to the capillaries in the NS and L-NAME groups ($P < 0.01$), whereas the L-NAME group had significantly shorter cortical capillaries than the NS group ($P < 0.01$) (**Figure 5B**).

Volume of the cortical capillaries: We also calculated the total volume of the cortical capillaries as 4.38 ± 1.52 mm^3 in the NS group, 8.81 ±

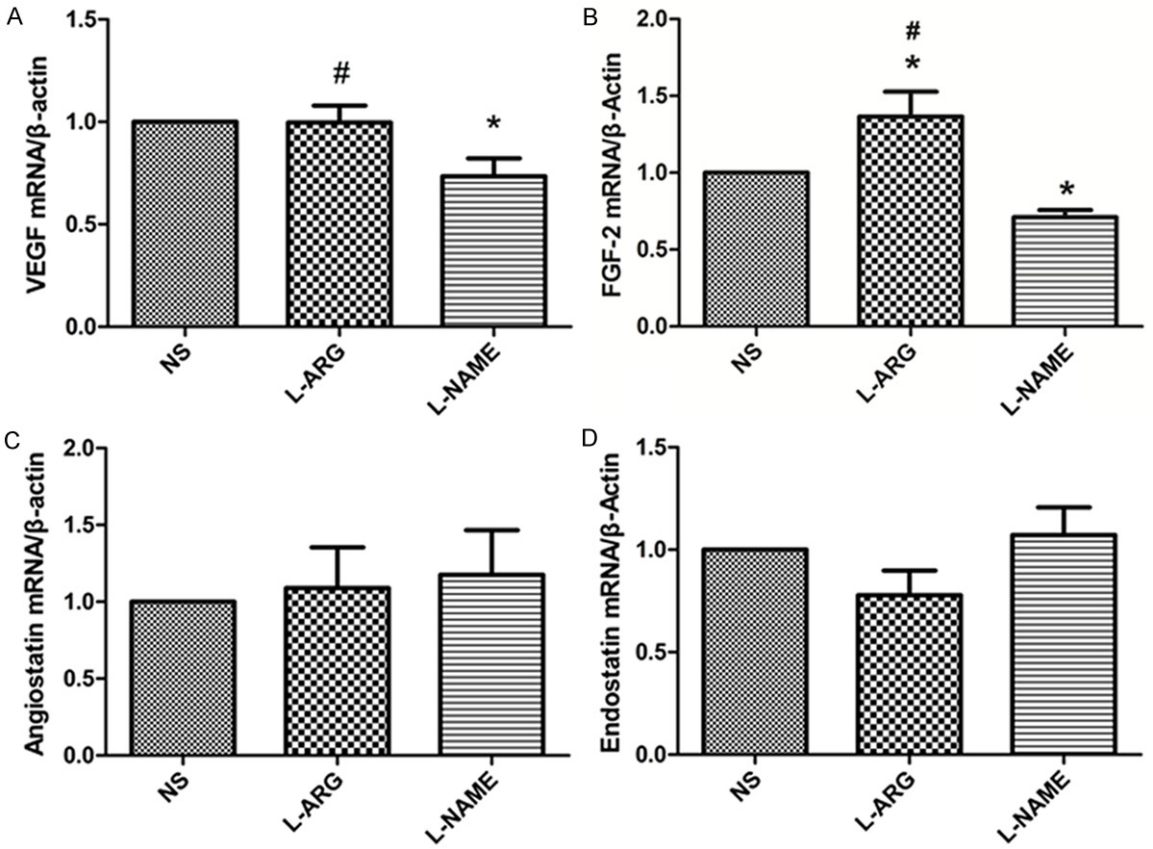

Figure 6. A. VEGF mRNA expression in the cerebral cortex was measured by qRT-PCR. B. Comparisons of FGF-2 expression in the cerebral cortex, as measured by qRT-PCR. C. Angiostatin expression in the cerebral cortex, as measured by qRT-PCR. D. Endostatin expression in the cerebral cortex, as measured by qRT-PCR. *indicates $P < 0.05$ vs. NS. #indicates $P < 0.05$ vs. L-NAME.

1.62 mm^3 in the L-ARG group, and 3.87 ± 0.55 mm^3 in the L-NAME group. The total volume of the cortical capillaries in the L-ARG group was significantly increased compared with the NS and L-NAME groups ($P < 0.01$) (**Figure 5C**).

Surface area of the cortical capillaries: We measured the total surface area of the cortical capillaries as 22.27 ± 4.24 cm^2 in the NS group, 52.05 ± 1.43 cm^2 in the L-ARG group, and 13.58 ± 1.53 cm^2 in the L-NAME group. The total surface area of the cortical capillaries in the L-ARG group was significantly larger than the capillaries in the NS and L-NAME groups ($P < 0.01$) (**Figure 5D**).

Real-time quantitative PCR

We measured VEGF expression to investigate the effect of inhibiting NO synthesis on the transcription of angiogenic factors. VEGF expression was significantly decreased in the L-NAME group compared with the NS group ($P < 0.05$). In contrast, VEGF expression in the L-ARG group was significantly increased compared with the L-NAME group ($P < 0.05$) (**Figure 6A**). The expression of the FGF-2 mRNA was significantly increased in the L-ARG group compared with the NS and L-NAME groups ($P < 0.05$). FGF-2 expression was significantly decreased in the L-NAME group compared with the NS group ($P < 0.05$) (**Figure 6B**). There were no significant differences in angiostatin and endostatin expression between the three groups ($P > 0.05$) (**Figure 6C**, **6D**).

Western blotting

The levels of the VEGF and FGF-2 proteins were significantly increased in the L-ARG group compared to the NS group ($P < 0.05$) (**Figure 7A**, **7B**). The expression of the FGF-2 protein was significantly decreased in the L-NAME group compared to the NS group (**Figure 7B**). There

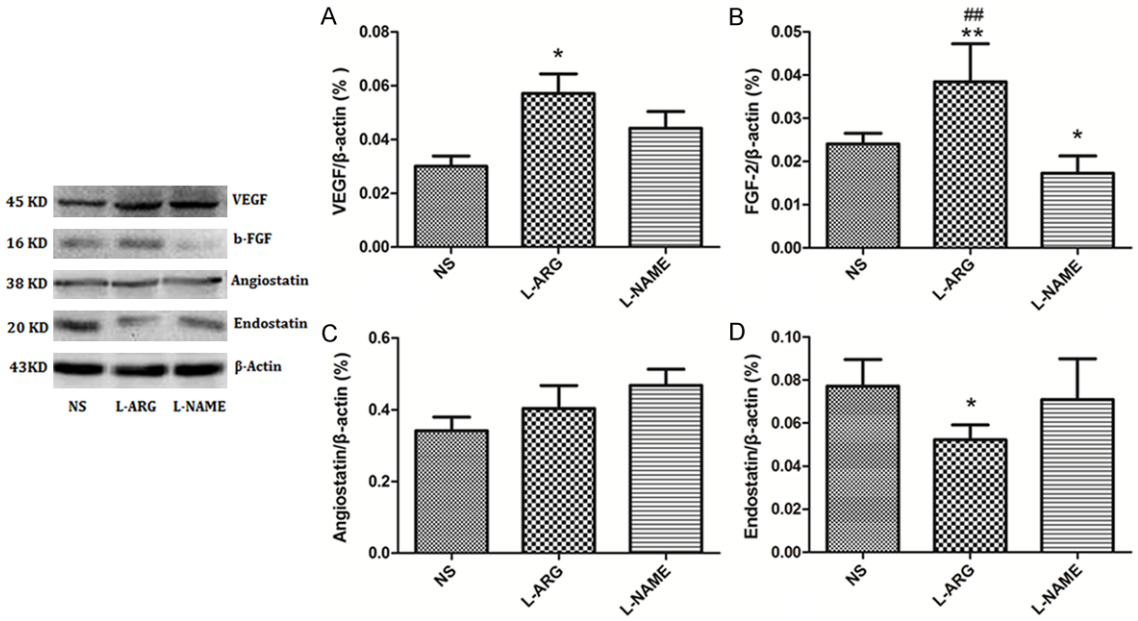

Figure 7. A. Western blot analysis of VEGF expression in the cerebral cortex. B. Western blot analysis of FGF-2 expression in the cerebral cortex. C. Western blot analysis of angiostatin expression in the cerebral cortex. D. Western blot analysis of endostatin expression in the cerebral cortex. *indicates $P < 0.05$ vs. NS, **indicates $P < 0.01$ vs. NS, ##indicates $P < 0.01$ vs. L-NAME.

were no differences in the levels of the angiostatin and endostatin protein levels in the L-NAME and NS groups (**Figure 7C**, **7D**); however, the levels of the endostatin protein were significantly decreased in the L-ARG-treated rats compared to the NS control rats ($P > 0.05$) (**Figure 7D**).

Discussion

In previous studies, the expression levels and the balance between angiogenic factors and angiogenesis inhibitors have been shown to determine the extent of blood vessel growth, and the NO signal pathway is essential for the regulation of these two classes of effectors [25, 41-43]. This study aimed to determine the effects and mechanism of nitric oxide on cerebral capillary angiogenesis, spatial learning, and memory ability in Sprague-Dawley rats. A 28-day i.c.v. injections of a low dose of the NO precursor L-ARG induced the long-term activation of NOS and improved memory retention. Moreover, a 28-day i.c.v. injections of a low dose of the NOS inhibitor L-NAME decreased NOS activity and impaired memory retention.

The times at which the L-ARG and L-NAME interventions were delivered and the methods used to assess spatial learning and memory in our study are not the same as those in previous reports. In the study by Wei, only a 7-day treatment period with i.c.v. injections of the NO precursor L-ARG and the NOS inhibitor L-NAME was examined [44]. As blood vessel growth is a relatively slow process, we administered L-ARG and L-NAME to rats for 28 days via an i.c.v. infusion to study cortical capillary angiogenesis more thoroughly. We also assessed spatial learning and memory with the Morris water maze instead of the Y-maze task. The Morris water maze is a relatively difficult task that is extremely sensitive to changes in spatial learning, and information on both working and reference memory can be extracted from the data.

Consistent with previous studies, the continuous long-term L-ARG and L-NAME treatments (28-day) reinforced or impaired brain function, respectively, in this study. The NO precursor L-ARG indeed affects the encoding of spatial information and attenuates recognition memory impairments in different animal models of cognitive impairment. Moreover, NO is involved in spatial recognition memory [45-47]. The use of different NOS inhibitors led to learning deficits that were counteracted by treatment with NO precursors [48]. The NO precursors molsi-

domine and NCX-2057 were able to affect distinct aspects of recognition, such as the acquisition, storage and retrieval of information [49]. Although we chose L-ARG as the NO precursor in the current study, which was not used in previous studies, our results are consistent with the results of previous studies. L-ARG improved the memory retention of rats treated with this NO precursor.

In previous studies, NOS inhibitors such as L-NAME decreased the NO concentration in the brain and impaired learning and memory performance in rats [50, 51]; our results are consistent with these reports. As claimed by previous studies, L-NAME has no effect or negative effects on memory at a lower dose range than described above [52-54]. Therefore, both NO precursors and NOS inhibitors regulate learning and memory ability and low-dose NO is involved in cognition and memory. We identified NO as a positive regulator of spatial learning and memory that exhibits an extremely variable role in memory formation.

Our research helps elucidate the structural bases for the positive effects of NO on brain functions. NO stimulates synaptic activity, neural plasticity and memory function [55, 56]. According to the vascular niche hypothesis, regeneration and repair via adult neurogenesis only occurs in an angiogenic environment, based on a complex interaction between the brain vasculature and neuronal function within the neurovascular unit [4, 5]. However, previous studies only measured capillary density, which may not allow changes in the total capillary number to be detected [43, 57, 58]. Because cortical capillaries are not arranged isotropically, researchers have not been able to accurately and easily quantify the cortical capillaries. In this paper, we evaluated the volume, length, and surface area of cortical capillaries using modern stereological methods. These measurements avoided the potential biases associated with density calculations. Moreover, we obtained isotropic, uniform random (IUR) sections using the isector technique to ensure that all cortical capillaries had an equal possibility of being sampled in all orientations [32]. In the current study, the results were clearly interpreted because we measured the total number of capillaries in the cortex.

The 28-day i.c.v. infusions of the NOS precursor of L-ARG or L-NAME induced changes in the cortical capillaries. The total volume, total length, and total surface area of the cortical capillaries in the L-ARG group were significantly higher. However, the cortical capillaries in the L-NAME group were significantly shorter, but L-NAME had no effect on the total volume or the total surface area of the cortical capillaries, Therefore, the main difference in neovascular vessel formation may only be visible in the length of the capillaries [59]. Thus, we speculate that the increase in the brain capillary parameters may be closely related to NO-induced alterations in brain functions.

In a previous study, the expression of the NOS isoform iNOS in feline mammary tumors was positively correlated with VEGF expression and microvessel density [60]. LNCaP cells express higher levels of eNOS, iNOS, and VEGF than BPH-1 cells, and L-NAME treatment reduced the expression of these genes [61]. In the study by Baum and colleagues, endothelial NOS was the main mediator of shear stress-dependent angiogenesis in skeletal muscle after prazocin administration [62]. Protocatechuic acid induced angiogenesis through the PI3K-Akt-eNOS-VEGF signaling pathway in a previous study [63]. Moreover, VEGF also regulates NO synthesis by regulating eNOS expression in glomerular endothelial cells [64]. Thus, NO and VEGF interact to promote endothelial cell proliferation, migration, tube formation and angiogenesis, although different NOS isoforms were examined in the studies. Our results strengthen the hypothesis that NO regulates the expression of VEGF as an upstream factor. Moreover, the impact of different NOS isoforms on VEGF expression must be examined further.

Although previous research showed that FGF-2 independently promotes angiogenesis and does not rely on NO, NO selectively enhances FGF-2 activity to induce mitosis in primary rat aortic smooth muscle cells and promote the repair of vascular injuries [65]. In mouse embryonic stem cells, α2-macroglobulin (α2M) improves angiogenesis by stimulating NO production and FGF-2 expression. L-NAME treatment inhibits this α2M-induced increase in FGF-2 expression and angiogenesis. Moreover, FGF-2 induced angiogenesis modulates angiotensin-converting enzyme inhibitor expression in the

coronary endothelium, but the NOS pathway inhibits this process [66]. As shown in our study, NO regulates FGF-2 expression in the rat cortex, consistent with previous reports.

Angiostatin has been reported to inhibit coronary angiogenesis when nitric oxide production is impaired in a coronary artery occlusion model in dog heart [57]. As reported in the study by Koshida, angiostatin decreases the association of heat shock protein 90 with eNOS in aortas and bovine aortic endothelial cell (BAEC) cultures and increases O_2 production in L-NAME-treated BAEC cells, thus altering endothelial function by allowing eNOS to generate O_2 [67]. Angiostatin impairs endothelium-dependent vasodilation and is regulated by NO. However, NO did not influence the angiostatin levels in the rat cortex after an i.c.v. infusion of L-NAME or L-ARG. We speculate that the differences in animal species, organs examined, and drug intervention time might explain the discrepancies between our results and previous reports.

As shown in a previous study, NO modulates endostatin expression and provides important new pharmacological information for the systemic induction of endogenous endostatin release by a common NO precursor [68]. Endostatin inhibits VEGF-induced endothelial cell migration and angiogenesis upstream of NO synthesis by dephosphorylating eNOS on Ser1177 [69]. Endostatin also uncouples NO and Ca^{2+} responses to bradykinin by increasing superoxide (O2*-) production in the intact coronary endothelium [70]. Moreover, endostatin blocks NO production and decreases VEGF and collagen XVIII levels in squamous carcinoma cells [71]. In addition, endostatin and NO each regulate the activity of the other, consistent with our results.

In our study, NO affected the levels of both angiopoietin and anti-angiogenesis factors in the L-ARG- and L-NAME-treated cells, and the change in the angiopoietin levels was particularly obvious. Angiogenesis, which is defined as the formation of new blood vessels from endothelial cells, is a complex process regulated by angiopoietin and anti-angiogenesis factors, together with other genetic and environmental factors [1-3]. We speculated that the change in the regulation angiogenesis-related factors may be closely related to the variations in the cortical capillaries observed after the NO treatment.

Our findings are consistent with the previous studies we described above, and the changes in the characteristics of cortical capillaries were consistent with the expression profiles of the growth factors VEGF and FGF-2. These results led us to speculate that the NO-induced changes in the cortical capillaries might be due to an indirect regulation of angiogenesis-related factors by NO itself.

In conclusion, we have provided evidence that the L-ARG treatment resulted in better memory retention skills and a more developed cortex capillary network, which were accompanied by the overexpression of VEGF, FGF-2 and angiostatin. Conversely, the L-NAME treatment was associated with impaired memory retention and reductions in the size of the blood vessel system, accompanied by reduced VEGF and FGF-2 expression. Based on our results, the NO-induced variations might be an important structural basis for the NO-induced changes in memory retention, thus confirming a role for NO in regulating angiogenesis in the cortex. Our results might also provide a baseline for further studies investigating NO-based treatments and intervention targets in brain capillaries.

Acknowledgements

This study was supported by the National Natural Science Foundation of China (NSFC, 81601967, 81171238, 31271288, and 31300985) and the Research Foundation for 100 Academic and Discipline Talented Leaders of Chongqing P. R. Chongqing Municipal Healthcare Department Medical Research Grant (No: 2010-1-20:2).

Disclosure of conflict of interest

None.

Address correspondence to: Yong Tang, Department of Histology and Embryology, Chongqing Medical University, Chongqing 400016, P. R. China. Tel: +86 023 68485633; Fax: +86 023 68485589; E-mail: ytang062@163.com

References

[1] Flamme I, Frolich T and Risau W. Molecular mechanisms of vasculogenesis and embryonic

angiogenesis. J Cell Physiol 1997; 173: 206-210.
[2] Risau W. Mechanisms of angiogenesis. Nature 1997; 386: 671-674.
[3] Folkman J and Shing Y. Angiogenesis. J Biol Chem 1992; 267: 10931-10934.
[4] Palmer TD, Willhoite AR and Gage FH. Vascular niche for adult hippocampal neurogenesis. J Comp Neurol 2000; 425: 479-494.
[5] Segura I, De Smet F, Hohensinner PJ, Ruiz de Almodovar C and Carmeliet P. The neurovascular link in health and disease: an update. Trends Mol Med 2009; 15: 439-451.
[6] Hanahan D and Folkman J. Patterns and emerging mechanisms of the angiogenic switch during tumorigenesis. Cell 1996; 86: 353-364.
[7] Foster RR, Hole R, Anderson K, Satchell SC, Coward RJ, Mathieson PW, Gillatt DA, Saleem MA, Bates DO and Harper SJ. Functional evidence that vascular endothelial growth factor may act as an autocrine factor on human podocytes. Am J Physiol Renal Physiol 2003; 284: F1263-1273.
[8] Matsuzaki H, Tamatani M, Yamaguchi A, Namikawa K, Kiyama H, Vitek MP, Mitsuda N and Tohyama M. Vascular endothelial growth factor rescues hippocampal neurons from glutamate-induced toxicity: signal transduction cascades. FASEB J 2001; 15: 1218-1220.
[9] Bachelder RE, Crago A, Chung J, Wendt MA, Shaw LM, Robinson G and Mercurio AM. Vascular endothelial growth factor is an autocrine survival factor for neuropilin-expressing breast carcinoma cells. Cancer Res 2001; 61: 5736-5740.
[10] Gualandris A, Urbinati C, Rusnati M, Ziche M and Presta M. Interaction of high-molecular-weight basic fibroblast growth factor with endothelium: biological activity and intracellular fate of human recombinant M(r) 24,000 bFGF. J Cell Physiol 1994; 161: 149-159.
[11] Tille JC, Wood J, Mandriota SJ, Schnell C, Ferrari S, Mestan J, Zhu Z, Witte L and Pepper MS. Vascular endothelial growth factor (VEGF) receptor-2 antagonists inhibit VEGF- and basic fibroblast growth factor-induced angiogenesis in vivo and in vitro. J Pharmacol Exp Ther 2001; 299: 1073-1085.
[12] Auguste P, Gursel DB, Lemiere S, Reimers D, Cuevas P, Carceller F, Di Santo JP and Bikfalvi A. Inhibition of fibroblast growth factor/fibroblast growth factor receptor activity in glioma cells impedes tumor growth by both angiogenesis-dependent and -independent mechanisms. Cancer Res 2001; 61: 1717-1726.
[13] Gabler C, Plath-Gabler A, Killian GJ, Berisha B and Schams D. Expression pattern of fibroblast growth factor (FGF) and vascular endothelial growth factor (VEGF) system members in bovine corpus luteum endothelial cells during treatment with FGF-2, VEGF or oestradiol. Reprod Domest Anim 2004; 39: 321-327.
[14] Tomanek RJ, Sandra A, Zheng W, Brock T, Bjercke RJ and Holifield JS. Vascular endothelial growth factor and basic fibroblast growth factor differentially modulate early postnatal coronary angiogenesis. Circ Res 2001; 88: 1135-1141.
[15] Castellon R, Hamdi HK, Sacerio I, Aoki AM, Kenney MC and Ljubimov AV. Effects of angiogenic growth factor combinations on retinal endothelial cells. Exp Eye Res 2002; 74: 523-535.
[16] Pepper MS and Mandriota SJ. Regulation of vascular endothelial growth factor receptor-2 (Flk-1) expression in vascular endothelial cells. Exp Cell Res 1998; 241: 414-425.
[17] Giavazzi R, Sennino B, Coltrini D, Garofalo A, Dossi R, Ronca R, Tosatti MP and Presta M. Distinct role of fibroblast growth factor-2 and vascular endothelial growth factor on tumor growth and angiogenesis. Am J Pathol 2003; 162: 1913-1926.
[18] Abdollahi A, Hahnfeldt P, Maercker C, Grone HJ, Debus J, Ansorge W, Folkman J, Hlatky L and Huber PE. Endostatin's antiangiogenic signaling network. Mol Cell 2004; 13: 649-663.
[19] Kruger EA, Duray PH, Tsokos MG, Venzon DJ, Libutti SK, Dixon SC, Rudek MA, Pluda J, Allegra C and Figg WD. Endostatin inhibits microvessel formation in the ex vivo rat aortic ring angiogenesis assay. Biochem Biophys Res Commun 2000; 268: 183-191.
[20] Taddei L, Chiarugi P, Brogelli L, Cirri P, Magnelli L, Raugei G, Ziche M, Granger HJ, Chiarugi V and Ramponi G. Inhibitory effect of full-length human endostatin on in vitro angiogenesis. Biochem Biophys Res Commun 1999; 263: 340-345.
[21] Wahl ML, Kenan DJ, Gonzalez-Gronow M and Pizzo SV. Angiostatin's molecular mechanism: aspects of specificity and regulation elucidated. J Cell Biochem 2005; 96: 242-261.
[22] Lee TY, Muschal S, Pravda EA, Folkman J, Abdollahi A and Javaherian K. Angiostatin regulates the expression of antiangiogenic and proapoptotic pathways via targeted inhibition of mitochondrial proteins. Blood 2009; 114: 1987-1998.
[23] Philippu A and Prast H. Role of histaminergic and cholinergic transmission in cognitive processes. Drug News Perspect 2001; 14: 523-529.
[24] Philippu A and Prast H. Importance of histamine in modulatory processes, locomotion and memory. Behav Brain Res 2001; 124: 151-159.

[25] Ziche M and Morbidelli L. Nitric oxide and angiogenesis. J Neurooncol 2000; 50: 139-148.
[26] Seddon M, Melikian N, Dworakowski R, Shabeeh H, Jiang B, Byrne J, Casadei B, Chowienczyk P and Shah AM. Effects of neuronal nitric oxide synthase on human coronary artery diameter and blood flow in vivo. Circulation 2009; 119: 2656-2662.
[27] Cooke JP and Losordo DW. Nitric oxide and angiogenesis. Circulation 2002; 105: 2133-2135.
[28] Szabo C, Ischiropoulos H and Radi R. Peroxynitrite: biochemistry, pathophysiology and development of therapeutics. Nat Rev Drug Discov 2007; 6: 662-680.
[29] Paxinos G, Watson CR and Emson PC. AChE-stained horizontal sections of the rat brain in stereotaxic coordinates. J Neurosci Methods 1980; 3: 129-149.
[30] Plech A, Klimkiewicz T and Maksym B. Effect of L-arginine on memory in rats. Pol J Pharmacol 2003; 55: 987-992.
[31] Qiang M, Chen YC, Wang R, Wu FM and Qiao JT. Nitric oxide is involved in the formation of learning and memory in rats: studies using passive avoidance response and Morris water maze task. Behav Pharmacol 1997; 8: 183-187.
[32] Wang S, Chen L, Zhang L, Huang C, Xiu Y, Wang F, Zhou C, Luo Y, Xiao Q and Tang Y. Effects of long-term exercise on spatial learning, memory ability, and cortical capillaries in aged rats. Med Sci Monit 2015; 21: 945-954.
[33] Wyss JM, Chambless BD, Kadish I and van Groen T. Age-related decline in water maze learning and memory in rats: strain differences. Neurobiol Aging 2000; 21: 671-681.
[34] Gundersen HJ and Jensen EB. The efficiency of systematic sampling in stereology and its prediction. J Microsc 1987; 147: 229-263.
[35] Tang Y and Nyengaard JR. A stereological method for estimating the total length and size of myelin fibers in human brain white matter. J Neurosci Methods 1997; 73: 193-200.
[36] Li C, Yang S, Chen L, Lu W, Qiu X, Gundersen HJ and Tang Y. Stereological methods for estimating the myelin sheaths of the myelinated fibers in white matter. Anat Rec (Hoboken) 2009; 292: 1648-1655.
[37] Huang CX, Qiu X, Wang S, Wu H, Xia L, Li C, Gao Y, Zhang L, Xiu Y, Chao F and Tang Y. Exercise-induced changes of the capillaries in the cortex of middle-aged rats. Neuroscience 2013; 233: 139-145.
[38] Gaspard GJ, MacLean J, Rioux D and Pasumarthi KB. A novel beta-adrenergic response element regulates both basal and agonist-induced expression of cyclin-dependent kinase 1 gene in cardiac fibroblasts. Am J Physiol Cell Physiol 2014; 306: C540-550.
[39] Feridooni T, Hotchkiss A, Remley-Carr S, Saga Y and Pasumarthi KB. Cardiomyocyte specific ablation of p53 is not sufficient to block doxorubicin induced cardiac fibrosis and associated cytoskeletal changes. PLoS One 2011; 6: e22801.
[40] Wafa K, MacLean J, Zhang F and Pasumarthi KB. Characterization of growth suppressive functions of a splice variant of cyclin D2. PLoS One 2013; 8: e53503.
[41] Pipili-Synetos E, Sakkoula E and Maragoudakis ME. Nitric oxide is involved in the regulation of angiogenesis. Br J Pharmacol 1993; 108: 855-857.
[42] Ziche M, Morbidelli L, Masini E, Amerini S, Granger HJ, Maggi CA, Geppetti P and Ledda F. Nitric oxide mediates angiogenesis in vivo and endothelial cell growth and migration in vitro promoted by substance P. J Clin Invest 1994; 94: 2036-2044.
[43] Zhang R, Wang L, Zhang L, Chen J, Zhu Z, Zhang Z and Chopp M. Nitric oxide enhances angiogenesis via the synthesis of vascular endothelial growth factor and cGMP after stroke in the rat. Circ Res 2003; 92: 308-313.
[44] Wei XM, Yang W, Liu LX and Qi WX. Effects of L-arginine and N(omega)-nitro-L-arginine methylester on learning and memory and alpha7 nAChR expression in the prefrontal cortex and hippocampus of rats. Neurosci Bull 2013; 29: 303-310.
[45] Pitsikas N, Zisopoulou S and Sakellaridis N. Nitric oxide donor molsidomine attenuates psychotomimetic effects of the NMDA receptor antagonist MK-801. J Neurosci Res 2006; 84: 299-305.
[46] Gourgiotis I, Kampouri NG, Koulouri V, Lempesis IG, Prasinou MD, Georgiadou G and Pitsikas N. Nitric oxide modulates apomorphine-induced recognition memory deficits in rats. Pharmacol Biochem Behav 2012; 102: 507-514.
[47] Pitsikas N. The nitric oxide (NO) donor molsidomine antagonizes scopolamine and L-NAME-induced performance deficits in a spatial memory task in the rat. Behav Brain Res 2009; 200: 160-164.
[48] Prast H and Philippu A. Nitric oxide as modulator of neuronal function. Prog Neurobiol 2001; 64: 51-68.
[49] Pitsikas N, Rigamonti AE, Cella SG and Muller EE. Effects of the nitric oxide donor molsidomine on different memory components as assessed in the object-recognition task in the rat. Psychopharmacology (Berl) 2002; 162: 239-245.
[50] Pitsikas N, Rigamonti AE, Bonomo SM, Cella SG and Muller EE. Molsidomine antagonizes L-NAME-induced acquisition deficits in a recogni-

tion memory task in the rat. Pharmacol Res 2003; 47: 311-315.
[51] Prickaerts J, Steinbusch HW, Smits JF and de Vente J. Possible role of nitric oxide-cyclic GMP pathway in object recognition memory: effects of 7-nitroindazole and zaprinast. Eur J Pharmacol 1997; 337: 125-136.
[52] Tamagnini F, Barker G, Warburton EC, Burattini C, Aicardi G and Bashir ZI. Nitric oxide-dependent long-term depression but not endocannabinoid-mediated long-term potentiation is crucial for visual recognition memory. J Physiol 2013; 591: 3963-3979.
[53] Boultadakis A, Georgiadou G and Pitsikas N. Effects of the nitric oxide synthase inhibitor L-NAME on different memory components as assessed in the object recognition task in the rat. Behav Brain Res 2010; 207: 208-214.
[54] Georgiadou G and Pitsikas N. Repeated administration of the nitric oxide synthase inhibitor l-NAME differentially affects rats' recognition memory. Behav Brain Res 2011; 224: 140-144.
[55] Calabrese V, Mancuso C, Calvani M, Rizzarelli E, Butterfield DA and Stella AM. Nitric oxide in the central nervous system: neuroprotection versus neurotoxicity. Nat Rev Neurosci 2007; 8: 766-775.
[56] Calabrese V, Guagliano E, Sapienza M, Panebianco M, Calafato S, Puleo E, Pennisi G, Mancuso C, Butterfield DA and Stella AG. Redox regulation of cellular stress response in aging and neurodegenerative disorders: role of vitagenes. Neurochem Res 2007; 32: 757-773.
[57] Matsunaga T, Weihrauch DW, Moniz MC, Tessmer J, Warltier DC and Chilian WM. Angiostatin inhibits coronary angiogenesis during impaired production of nitric oxide. Circulation 2002; 105: 2185-2191.
[58] Gertz K, Priller J, Kronenberg G, Fink KB, Winter B, Schrock H, Ji S, Milosevic M, Harms C, Bohm M, Dirnagl U, Laufs U and Endres M. Physical activity improves long-term stroke outcome via endothelial nitric oxide synthase-dependent augmentation of neovascularization and cerebral blood flow. Circ Res 2006; 99: 1132-1140.
[59] Whiteus C, Freitas C and Grutzendler J. Perturbed neural activity disrupts cerebral angiogenesis during a postnatal critical period. Nature 2014; 505: 407-411.
[60] Islam MS, Matsumoto M, Hidaka R, Miyoshi N and Yasuda N. Expression of NOS and VEGF in feline mammary tumours and their correlation with angiogenesis. Vet J 2012; 192: 338-344.
[61] Vanella L, Di Giacomo C, Acquaviva R, Santangelo R, Cardile V, Barbagallo I, Abraham NG and Sorrenti V. The DDAH/NOS pathway in human prostatic cancer cell lines: antiangiogenic effect of L-NAME. Int J Oncol 2011; 39: 1303-1310.
[62] Baum O, Da Silva-Azevedo L, Willerding G, Wockel A, Planitzer G, Gossrau R, Pries AR and Zakrzewicz A. Endothelial NOS is main mediator for shear stress-dependent angiogenesis in skeletal muscle after prazosin administration. Am J Physiol Heart Circ Physiol 2004; 287: H2300-2308.
[63] Kang Z, Zhu H, Jiang W and Zhang S. Protocatechuic acid induces angiogenesis through PI3K-Akt-eNOS-VEGF signalling pathway. Basic Clin Pharmacol Toxicol 2013; 113: 221-227.
[64] Feliers D, Chen X, Akis N, Choudhury GG, Madaio M and Kasinath BS. VEGF regulation of endothelial nitric oxide synthase in glomerular endothelial cells. Kidney Int 2005; 68: 1648-1659.
[65] Hassid A, Arabshahi H, Bourcier T, Dhaunsi GS and Matthews C. Nitric oxide selectively amplifies FGF-2-induced mitogenesis in primary rat aortic smooth muscle cells. Am J Physiol 1994; 267: H1040-1048.
[66] Donnini S, Solito R, Giachetti A, Granger HJ, Ziche M and Morbidelli L. Fibroblast growth factor-2 mediates Angiotensin-converting enzyme inhibitor-induced angiogenesis in coronary endothelium. J Pharmacol Exp Ther 2006; 319: 515-522.
[67] Koshida R, Ou J, Matsunaga T, Chilian WM, Oldham KT, Ackerman AW and Pritchard KA Jr. Angiostatin: a negative regulator of endothelial-dependent vasodilation. Circulation 2003; 107: 803-806.
[68] Deininger MH, Wybranietz WA, Graepler FT, Lauer UM, Meyermann R and Schluesener HJ. Endothelial endostatin release is induced by general cell stress and modulated by the nitric oxide/cGMP pathway. FASEB J 2003; 17: 1267-1276.
[69] Urbich C, Reissner A, Chavakis E, Dernbach E, Haendeler J, Fleming I, Zeiher AM, Kaszkin M and Dimmeler S. Dephosphorylation of endothelial nitric oxide synthase contributes to the anti-angiogenic effects of endostatin. FASEB J 2002; 16: 706-708.
[70] Zhang AY, Teggatz EG, Zou AP, Campbell WB and Li PL. Endostatin uncouples NO and Ca2+ response to bradykinin through enhanced O2*- production in the intact coronary endothelium. Am J Physiol Heart Circ Physiol 2005; 288: H686-694.
[71] Hebert C, Siavash H, Norris K, Nikitakis NG and Sauk JJ. Endostatin inhibits nitric oxide and diminishes VEGF and collagen XVIII in squamous carcinoma cells. Int J Cancer 2005; 114: 195-201.